

## Article

# Harvest Stage Recognition and Potential Fruit Damage Indicator for Berries based on Hidden Markov Models and the Viterbi Algorithm

Marcos E. Orchard <sup>1,3,†</sup> , Carlos Muñoz <sup>1,\*†</sup> , Juan Ignacio Huircan <sup>1</sup>, Patricio Galeas <sup>2,†</sup>  and Heraldo Rozas <sup>3,†</sup>,

<sup>1</sup> Department of Electrical Engineering, Universidad de La Frontera, Temuco 4811230, Chile; juan.huircan@ufrontera.cl

<sup>2</sup> Department of Computer Science, Universidad de La Frontera, Temuco 4811230, Chile; patricio.galeas@ufrontera.cl

<sup>3</sup> Department of Electrical Engineering, Faculty of Physical and Mathematical Sciences, Universidad de Chile, Santiago, Chile; morchard@ing.uchile.cl (M.O.); hrozas@ing.uchile.cl (H.R.)

\* Correspondence: carlos.munoz@ufrontera.cl; Tel.: +56-45-232-5531

† These authors contributed equally to this work.

**Abstract:** This article proposes a monitoring system that allows to track transitions between different stages in the berry harvesting process (berry picking, waiting for transport, transport, and arrival to the packing) solely using information from temperature and vibration sensors located in the basket. The monitoring system assumes a characterization of the process based on Hidden Markov Models and uses the Viterbi algorithm to perform inference and estimate the most likely state trajectory. The obtained state trajectory estimate is then used to compute a potential damage indicator in real-time. The proposed methodology does not require information about the weight of the basket to identify each of the different stages, which makes it effective and more efficient than other alternatives available in the industry.

**Keywords:** Berry harvesting stages; Markov chains; Viterbi algorithm; monitoring; fruit damage indicator.

## 1. Introduction

Chile is the main exporter of fresh fruit in the Southern Hemisphere (ODEPA), generating 59.3% of the total production [1]. Worldwide, Chile exports more than 75 different species to more than 100 countries around the world, being a leader in the export of table grapes, plums, apples, blueberries and peaches. In this regard, any improvement in productive processes of fresh fruit harvesting for exportation has a significant impact on the national economy. Those improvements should help to efficiently manage the whole chain of the productive process: crop, harvest, packing, and transport to the destination market.

The fruit produced in Chile, is mainly harvested manually (hand picking), but this process requires numerous personnel. Although the personnel working in harvesting processes is continuously trained, the vast majority of these workers are employed solely during the productive season. The coordination of this activity requires highly trained personnel in the process of manual harvest, since the fruit can suffer damage, mainly mechanical. Indeed, authors such as Li et al. [2] state that fresh fruit is susceptible to mechanical damage during the whole process, from harvesting in the harvest stage, the transfer to the

24 packing, its passage through it, and also during the transport that takes it to its final destination. This  
25 produces a decline in its quality and, therefore, economic damage. In strawberry studies, 51% of this  
26 damage occurs in the harvesting operation, 32% in transport to the destination market and only 17% in  
27 packing [3]. Several researchers have proposed that the mechanical damage in the fruit is given by three  
28 factors: the impact, the vibration and the pressure by the weight of the fruit [4], [5]. In the case of cherry,  
29 the processes that cause the loss of quality are three times faster at 20°C than at 10°C, and hence the  
30 importance of placing them fast in cooling chambers when the harvest temperature is high. For its part,  
31 [6] states that the damage in the cranberry is a product of mechanical damage and storage temperature.  
32 However, according to authors in [7], the definition of mechanical damage is not completely clear and  
33 the authors give different definitions. However, there is a general coincidence: mechanical damage is  
34 caused by one or more types of load (shock or load pressure) [8,9]. In this way, [10] described two different  
35 types of mechanical damage during post-harvest handling: (a) impacts during the process of harvesting,  
36 selecting, handling and transporting the fruit; and (b) compression loads during packing or storage lines.

37 In the post-harvest stage, from the packing to the destination markets, solutions for the monitoring  
38 and monitoring of agricultural products mainly aim at measuring the humidity and temperature within  
39 the transport vehicles. These studies incorporate Global Positioning Systems (GPSs) to pinpoint the  
40 location of the transport vehicle, General Packet Radio Services (GPRSs) for the communication of the  
41 transport vehicle with the monitoring station, and the use of Radio Frequency Identification (RFID) for  
42 the identification of the products [11]. Some of these technological solutions are commercially available,  
43 guaranteeing that the fruit will be transported under appropriate conditions and following the schedule  
44 committed by the company. Logistics during the harvest stage, however, are much more difficult to  
45 monitor, due to the relatively small number of personnel assigned to supervision tasks compared to the  
46 large number workers associated.

47 Ampatzidis et al., [12,13] addresses the problem of the integration of technologies in fruit orchards,  
48 with the inclusion of Radio Frequency Identification (RFID) technology and bar codes in harvest bins  
49 and orchard trees of cherries. With the help of an electronic scale and Differential Global Positioning  
50 Systems (DGPSs) in the tractors that transport the harvest bins, measurements of the weight associated  
51 with the harvested fruit are efficiently acquired. This allows to establish productivity indicators of the  
52 orchards and harvest personnel. This research effort recognizes that the weighing process, by means of an  
53 electronic scale on the tractor that transports the recollection bins, increases the loading time by almost  
54 33%, and proposes to solve this issue by acquiring these measurements directly at harvesting baskets  
55 automatically. However, this strategy does not take into account the fact that losses in the logistics chain,  
56 and the management of resources, are also related to the harvest personnel.

57 Some orchards in Chile use bar code technologies to identify the harvest baskets and the personnel  
58 that collect the fruit, by recording the number of baskets used by each collector and the time between  
59 each full basket delivery. However, the collected data does not provide information about the damage  
60 underwent by the fruit during this process [7]. Moreover, this approach does not consider relevant  
61 variables such as temperature and vibrations during harvesting, which can produce mechanical damage  
62 to the fruit, accelerating the dehydration process and finally decreasing the shelf life of the product.

63 Galeas et al. [14] presented a low complexity prototype of a basket with built-in sensors of weight,  
64 vibrations, and temperature. The main result was the identification of transition stages of the basket based  
65 only on the signals acquired. The transition stages shown useful to identify the time that the basket is in  
66 fruit picking, in waiting for transportation, in transportation to the packing and in the packing. Some  
67 of the sensors used were low-cost and not invasive, such as the IMUs and temperature, because they  
68 are based on MicroElectroMechanical (MEM) devices; however, the weight sensor requires supporting  
69 the strain gauges with mechanical parts inside the harvest basket, impacting directly on the fabrication  
70 costs. This design needs improvement by finding a way of removing the mechanical component without

71 compromising the functionality of the basket. To achieve this development is required to identify the  
 72 harvest's time transitions without using the fruit's weight. Length of the time elapsed by each one of the  
 73 harvest phases are useful to avoid high temperatures during prolonged periods of waiting times.

74 Time transition identification is a challenging problem, in particular for this settling because, as is  
 75 shown in Galeas [14], the harvest phases go sequentially, and due the data provided is gathered from  
 76 low-cost instrumentation, the problem is well suited for the use of Hidden Markov Chains methods, and  
 77 following the work of Rabiner [15], for this particular problem the Viterbi algorithm is one of the best  
 78 suited.

79 In this regard, the objective of this article is to propose a novel monitoring system for berry harvesting  
 80 processes that is solely based on the use of temperature and vibration sensors to perform inference and  
 81 estimate the most likely trajectory and switch times between each harvesting process stage. The obtained  
 82 trajectory estimate will be then used to compute a potential damage indicator for the fruit in terms both of  
 83 the registered temperature and vibration energy.

84 The article structure is as follows. Section 2 focuses on providing theoretical background on Markov  
 85 Chains and the Viterbi algorithm. Section 3.4 presents a description of the experimental setup that allowed  
 86 to acquire real-time vibration and temperature measurements directly from berry harvesting bins (i.e., the  
 87 *Smartbins*) and the proposed methodology for online recognition of different harvesting stages, as well as  
 88 the definition of a potential fruit damage indicator. Section 4 shows an analysis of the obtained results in  
 89 terms of data acquired from a field experimental campaign and Section 5 presents main conclusions of this  
 90 research effort.

## 91 2. Theoretical Background

### 92 2.1. Markov Chains

93 The proposed harvesting stage detection algorithm is built on the assumption that this sequence of  
 94 stages can be modeled as a Hidden Markov Model (HMM). Before going into the details that support this  
 95 assumption, though, it is important to define the concept of a first-order Markov Process. A Markov process  
 96 is a stochastic process that satisfies the Markov property (sometimes characterized as "memorylessness"),  
 97 that basically states that one can make predictions for the future of the process based solely on its present  
 98 state; i.e., conditional on the present state of the system, its future and past states are independent [15].

99 A first-order Markov Chain is a particular case of a Markov Process [15]. To define it properly, let us  
 100 consider a system such that its condition at any time instant can be characterized by a finite set of states  
 101  $S_1, S_2, \dots, S_N$ . At any time, this system can change its operational condition in time (i.e., the system makes  
 102 a transition from one "state" to another), with transition probabilities that are conditional to the current  
 103 state. We denote the state transition times as  $t = 1, \dots$ , and the state at any given time  $t$  as  $q_t$  [15].

104 The probabilistic model for system state transitions for the specific case of a discrete first-order Markov  
 105 Chain is completely described by the State Transition Matrix  $A$  and the initial state probability distribution  
 106  $\Pi$ , where:

$$P[q_t = S_j | q_{t-1} = S_i] = a_{ij}, \quad 1 \leq i, j \leq N, \quad (1)$$

107 and where:

- 108 •  $a_{ij} \geq 0$
- 109 •  $\sum_{j=1}^N a_{ij} = 1$ .

110 This Markov Process is denominated "observable" since the system output is a state that can be  
 111 directly measured. The probability of a given sequence can be computed in this case using the following  
 112 straightforward procedure:

$$P(O = \{S_{n_0}, S_{n_1}, \dots, S_{n_l}\} | Model) = P[S_{n_0}] \cdot P[S_{n_1} | S_{n_0}] \cdots P[S_{n_l} | S_{n_{l-1}}] \\ = \pi_0(n_0) \cdot a_{n_0 n_1} \cdots a_{n_{l-1} n_l} \quad (2)$$

113 Figure 1 shows a graphical representation of a single realization of this stochastic process. Please note  
 114 that state transition probabilities are completely determined by the current system state [15].

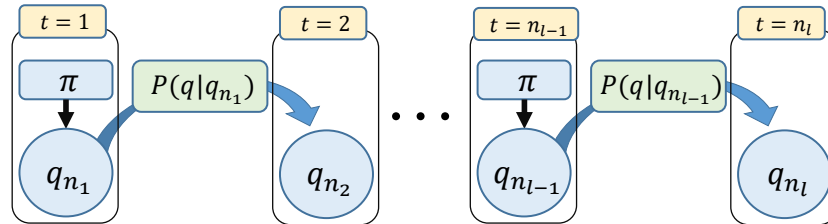


Figure 1. Graphical representation of a first-order Markov Chain realization.

## 115 2.2. Hidden Markov Models (HMMs)

116 In many practical cases, the system state cannot be directly measured and must be estimated. These  
 117 cases can be well characterized through the concept of Hidden Markov Models (HMMs). The adjective  
 118 "hidden" refers to the state sequence through which the model passes, not to the parameters of the  
 119 model; the model is still referred to as a hidden Markov model even if these parameters are known  
 120 exactly. Measurements are linked to the system states via a conditional probability density function. As  
 121 a consequence, the resulting model has two sources of uncertainty that affect the inference problem: (i)  
 122 hidden state dynamics and (ii) measurement noise [15].

123 A discrete HMM is characterized by the following parameters:

- 124 • N: Number of states. The set of possible states can be denoted by  $S = \{s_1, \dots, S_N\}$ . The state of the  
 125 system at time  $t$  is denoted  $q_t$ .
- 126 • M: Number of measurements associated with each state. Each measurement corresponds to a  
 127 physical outcome from the system that can be acquired using appropriate sensors.
- 128 • The transition probability distribution between system states  $A = \{a_{ij}\}$  where:

$$P[q_t = S_j | q_{t-1} = S_i] = a_{ij}, \quad 1 \leq i, j \leq N \quad (3)$$

129 • The measurement probability distribution conditional on the state  $j$ ,  $B = \{b_j(k)\}$ :

$$b_j(k) = P[O_k | q_t = S_j], \quad 1 \leq j \leq N \\ 1 \leq k \leq M \quad (4)$$

130 • The initial probability distribution of system states  $\pi$ , where:

$$\pi_i = P[q_1 = S_i]; \quad 1 \leq i, j \leq N \quad (5)$$

131 Considering all of the above, for convenience the following compact notation is typically used to  
 132 denote the entire set of parameters that characterizes the HMM:

$$\lambda = (A, B, \pi) \quad (6)$$

133 A realization of a HMM is graphically depicted in Figure 2. It is important to note that part of  
 134 the system dynamics are hidden to the observer ("hidden evolution model"). These dynamics follow a  
 135 similar pattern as the one depicted in Figure 1. In addition, in a HMM there is an observational model,  
 136 which is conditional on the state trajectory. The objective in an inference problem based on HMMs is to  
 137 estimate the sequence of hidden states  $S = \{s_1, \dots, S_N\}$  conditional on a set of system measurements  
 138  $O = \{O_1, \dots, O_N\}$  [15].

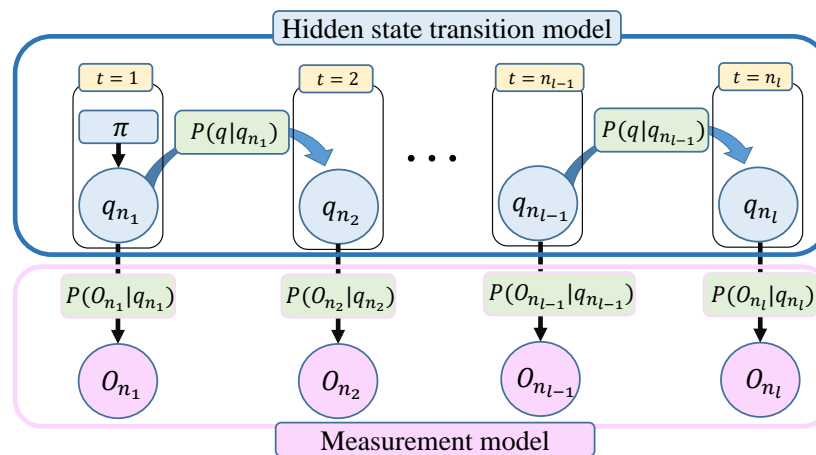


Figure 2. Graphical representation of a discrete HMM.

139 2.3. Viterbi Algorithm

140 The Viterbi Algorithm (VA) [16], [17], [18] was proposed as a solution to the decoding of convolutional  
 141 codes by Andrew J. Viterbi in 1967. This algorithm had a great impact in the fields of communications  
 142 and signal processing, extending its influence to other domains such as the problem of state estimation  
 143 in stochastic nonlinear systems. The Viterbi Algorithm (VA) aims at finding the optimal estimate for a  
 144 sequence of hidden states (called the Viterbi path) in a HMMs, conditional on a set of system measurements.  
 145 This task is achieved using a dynamic programming formulation, where the inference problem is divided  
 146 in a series of small stages (indexed by the time associated with each observation). At each stage, the VA  
 147 finds the optimal value for the state within the sequence, and it continues the analysis to the next stage in  
 148 an inductive manner. Formally speaking, to find the optimal sequence of hidden states  $Q^* = \{q_1^* q_2^* \dots q_T^*\}$   
 149 in a realization of a HMM, conditional on a sequence of system measurements  $O = \{O_1 O_2 \dots O_T\}$ , the  
 150 following variable is defined: [15,16]:

$$\delta_t(i) = \max_{q_1, q_2, \dots, q_{t-1}} P[q_1, q_2, \dots, q_{t-1}, O_1 O_2 \dots O_T | \lambda], \quad (7)$$

151 where  $\delta_t(i)$  is the most likely path for the HMM at time  $t$ , considering the first  $t$  observations and the state  
 152  $S_i$  as terminal condition. By induction, it is possible to write:

$$\delta_{t+1}(i) = [\max_i \delta_t(i) a_{ij}] \cdot B_j(O_{t+1}). \quad (8)$$

153 Therefore, the inference problem can now be solved in an iterative manner by running the following  
 154 the Pseudo-code:

---

**Algorithm 1** Viterbi Algorithm( $\lambda = (A, B, \pi), O$ )
 

---

**Inputs:**  $\lambda = (A, B, \pi), O$   
**Output:**  $Q^* = \{q_1^*, q_2^*, \dots, q_T^*\}$

```

1: for  $i = 1, \dots, N$  do ▷ Initialization
2:    $\delta_1(i) = \pi_i b_i(O_1)$ 
3:    $\psi_1(i) = 0$ 
4: for  $j = 1, \dots, N, t = 2, \dots, T$  do ▷ Recursion
5:    $\delta_t(j) = \max_{1 \leq i \leq N} [\delta_{t-1}(i) a_{ij}] \cdot B_j(O_t)$ 
6:    $\psi_t(i) = \operatorname{argmax}_{1 \leq i \leq N} [\delta_{t-1}(i) a_{ij}]$ 
7:    $P^* = \max_{1 \leq i \leq N} [\delta_T(i)]$ 
8:    $q_T^* = \operatorname{argmax}_{1 \leq i \leq N} [\delta_T(i)]$ 
9: for  $t = T-1, T-2, \dots, 1$  do ▷ Reconstruct state sequence
10:   $q_t^* = \psi_{t+1}(q_{t+1}^*)$ 
11: return  $Q^*$ 

```

---

155 **3. Materials and Methods**

156 **3.1. The Blueberry Harvesting Process**

157 The experiment is carried out inside the Boldo S.A. orchard. This orchard has 50 hectares planted  
 158 with blueberries and is located in Yungay, Chile, in coordinates Lat:  $-37.1149584$ , Long:  $-72.1973101$ .  
 159 As shown in Figure 3, its packing is located at the center of the garden and there are roads that divide  
 160 the plantation of blueberries into 3 sectors and each of these sectors is divided into 7 sub-sectors for the  
 161 irrigation process. Each sector has different varieties, including: Duke, Rabiteye, Brightwell, Tifblue,  
 162 O'Neal and Brigitta.

163 The process of picking fresh blueberries is done manually and begins by assigning a crew of collectors  
 164 in each sector of the garden (see Figure 4). The collectors walk through the orchard arranged in rows  
 165 of approximately 100 meters in length, provided with a plastic box of 3.5 liters hung from the neck by a  
 166 harness. The harvesting process has a duration of 20 to 40 minutes depending on the experience of the  
 167 harvester and how much fruit is in the bushes. Once filled the plastic box, the collector goes to the first  
 168 storage center (place provided with shade to temporally store the boxes previous to delivery at the local  
 169 packing site). In the reception center, another worker increase the accounting of the number of boxes  
 170 harvested by the collector and records the time when it was received. Finally the collector is provided  
 171 with an empty box to restart the picking process.

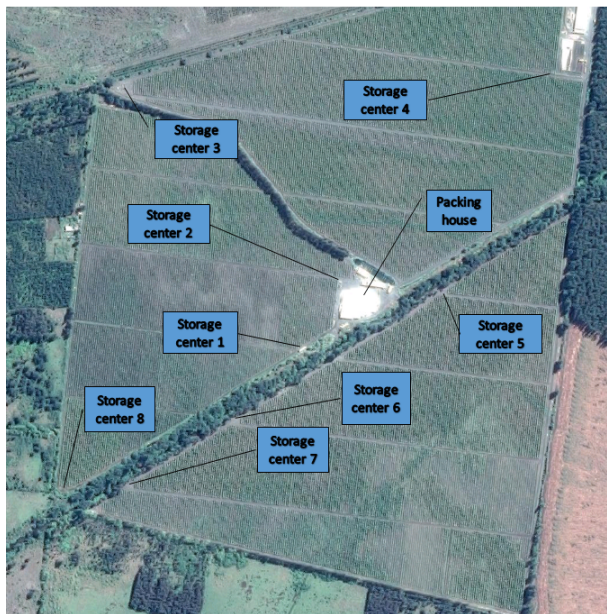


**Figure 3.** Blueberry orchard in Yungay, Chile.



**Figure 4.** Picture of the blueberry orchard.

172 The boxes full of fruit are stored in this storage center awaiting for a truck with a trailer to take them  
173 to the local packing site. Once arrived to the packing the net weight of fruit picked is recorded using an  
174 electronic scale. Then, the filled boxes are entered into the packing throughout a freezing tunnel to lower  
175 the temperature of the berries. Inside the packing, the boxes are emptied over a classification table and the  
176 boxes are recycled to begin a new harvest cycle.

177 *3.2. A Modular Distributed Monitoring System for the Harvesting Process: The "Smartbin"*

178 The proposed system has was developed, using a harvest basket of 3.5L, which incorporated two  
179 components:

180 - A main device installed on one of its sides, which contains a SODAQ Autonomous microcontroller  
181 card, real-time clock, temperature sensors and an inertial unit (IMU) to measure the vibrations of the  
182 harvest basket and detect the shocks suffered by it. - A false base sustained with a load cell, to measure at  
183 all times the weight carried by the basket.

184 The stand-alone SODAQ card uses an Atmel SAMD21J18 processor, with 256kb of Flash memory,  
185 32kb of SRAM memory and a 32-bit processor running at 48Mhz. In addition, it has a socket for the use of  
186 a micro SD card, which allows internal storage of the data. A real-time clock (DS1307) with the time and  
187 date was added to this device, information that is attached to each captured data. The IMU used is based  
188 on the MPU-9250 chip with accelerometer, gyroscope and 3-axis magnetometer. The unit also has two  
189 temperature sensors based on the digital device DS18B20, whose accuracy is 0.5°C. These temperature  
190 sensors protrude like two tubes of the main device, glued to one of the internal walls of the harvest box  
191 to measure the temperature of the berries at two heights, 6cm and 10cm from the base of the box (see  
192 Figure 5). The load cell located in the false base of the box is connected to an analog / digital converter  
193 HX711 which in turn is connected to the autonomous SODAQ device. The system was provided with a  
194 Li-Ion battery of 2300mAh/3.7V, for its energy autonomy, which was estimated at 30 hours of continuous  
195 operation.

196 This main device works as a remote collection unit and as a data logger, transmitting wireless and  
197 storing all the data collected in an SD Card installed in the Autonomous SODAQ card, with two types of  
198 records, one that is written every 100 ms with the measurements of the IMU, date and time, and another  
199 that is written every 15 seconds with measurements of temperature, weight, voltage of the battery, date  
200 and time. These time measurements are taken to identify faults in the system, and correlate the tests with  
201 the events that occurred during the day.



Figure 5. conditioned basket to on line measure of weight, 2 temperatures and accelerations.

202 3.3. Data acquisition campaign

203 Data from the experimental campaign was acquired using 5 "Smartbins" in an experimental set up  
204 carried out during one day in the middle of the harvest season of blueberries in the "El Boldo" orchard  
205 (see Figure 3). Each one of the 5 "Smartbins" was used in two consecutive harvest cycles during the day of  
206 the experiment. As a result, it was possible to record 10 complete harvesting cycles (each cycle finishes  
207 with the bin returned in the hands of the picker after being emptied). The structure of the acquired data  
208 set can be summarized as follows:

209 • *Temp\_1*: Temperature measurement acquired every 15 seconds using a sensor that is located near  
210 the bottom of the bin.

- 211 •  $Temp\_2$ : Temperature measurement acquired every 15 seconds using a sensor that is located near  
212 one of the four the external edges of the bin.
- 213 •  $Acc_x$ : Acceleration measurement in  $x$ -axis acquired ten times per second with an IMU located inside  
214 the bin.
- 215 •  $Acc_y$ : Acceleration measurement in  $y$ -axis acquired ten times per second with an IMU located inside  
216 the bin.
- 217 •  $Acc_z$ : Acceleration measurement in  $z$ -axis acquired ten times per second with an IMU located inside  
218 the bin.
- 219 •  $Weight$ : Net weight of the "Smartbin" acquired every 15 seconds with sensor that is located at the  
220 bottom of the bin.

221 In terms of nomenclature, and for all practical purposes, each harvesting cycle was labelled using the  
222 following format:  $N_i c_j$ , where  $i = 1, 2, 3, 4, 5$  refers to the  $i^{th}$  bin and  $j = 1, 2$  indicates the number of the  
223 recorded cycle for that specific bin.

224 Eight of these cycles  $N_i c_j$ , where  $i = 2, 3, 4, 5, j = 1, 2$  were used as training data, while two cycles  
225 where used for validation purposes ( $N_1 c_1$  and  $N_1 c_2$ , both corresponding to the 1<sup>st</sup> bin).

### 226 3.4. Proposed Methodology for Online Harvesting Stage Detection

227 The proposed methodology uses the Viterbi algorithm to perform inference of data sets and estimate  
228 the most likely state trajectory in the harvesting process. Indeed, this case study allows to define a finite  
229 number of possible "states" (each one associated with one stage of the harvesting procedure), making it a  
230 perfect candidate for the implementation of inference schemes based on the assumption of HMMs. The set  
231 of observations  $O$  incorporate data from IMUs and temperature sensors. Although the entire process has  
232 six "states" that can be identified (picking, waiting, transport (full bin), cooling, emptying, and transport  
233 (empty bin)), only four of them are hereby considered. The latter, since solely the first 4 states are critical in  
234 terms of quantifying the potential damage to the fruit during the harvesting procedure (the "emptying"  
235 state is fully automated, and afterwards the bin is empty). These states are:

- 236 1) **"Picking"** (S1): The pickers, provided with a 3.5 liter plastic box hung around the neck by a harness,  
237 cover the orchard prepared in rows approximately 100 meters long. Picking lasts 20 to 40 minutes  
238 per box, depending on the picker's experience and the volume of fruit on the shrubs. During this  
239 stage it is possible to measure high energy vibration signals and high temperatures.
- 240 2) **"Wait"** (S2): When the box is full, the picker goes to the storing center (shaded area), where he/she  
241 delivers the box for counting. The full boxes remain at the warehouse waiting for the tractor-trailer  
242 to take them to the local packing area.
- 243 3) **"Transport"** (full bin) (S3): The tractor-trailer transports full boxes from the warehouse to the local  
244 packing area.
- 245 4) **"Cooling"** (freezer tunnel) (S4): The fruit is admitted to packing via a conveyor table, where a  
246 cooling system lowers its temperature using a freezing tunnel.

247 Considering all of the above, a HMM is trained for this case study using eight harvesting cycles  
248  $N_i c_j$ , where  $i = 2, 3, 4, 5, j = 1, 2$ . Ground truth for the transition times between states in training (and  
249 also validation) data was defined by incorporating information acquired from the weight sensor that is  
250 located at the bottom of the "Smartbin". Weight sensor measurements allow to simplify the detection of  
251 state transitions because they help to determine the moment when the "Picking" stage is over (bin weight  
252 measurements stabilize at a constant value, a condition that can be tested by a basic hypothesis testing  
253 procedure), as well as the exact moment when the bin is emptied. Conditional to the latter transition  
254 times, it is possible to discriminate the "cooling" stage just by detecting sudden drops in temperature

255 measurements, while "wait" and "transport" stages can be identified since they differ significantly in terms  
 256 of the associated energy in the IMU signal.

257 The challenge behind the proposed method for state transition detection is to avoid the usage of  
 258 weight measurements altogether (except, as in this case study, for purposes of determining ground truth  
 259 transition times in training data). The latter since it would be preferable and significantly cheaper to  
 260 eliminate this weight sensor from the original design of the "Smartbin". For this purpose, a HMM is  
 261 conceived to describe the transition between the stages of the harvesting process, where the observation  
 262 space is solely determined by the following sensor information:

- 1) **Inertial Measurement Unit (IMU):** data acquired by the IMU. A simple pre-processing algorithm is implemented to complement this information with an average of the total energy in the vibration signal every 15[s] over the time window containing the last 15 seconds of measures.

$$IMU\_Energy_t = \sum_{j=t-14}^t acc_x(j)^2 + acc_y(j)^2 + acc_z(j)^2 \quad (9)$$

- 2) **Temperature Measurements:** Besides the information provided by sensors *Temp\_1* and *Temp\_2*, a simple pre-processing algorithm is implemented to measure the difference in readings between both temperature sensors.

$$Delta\_T(t) = Temp\_2(t) - Temp\_1(t) \quad (10)$$

263 Considering all of the above, and following the maximum likelihood estimation procedure explained  
 264 in [15] to determine the coefficients of state transition matrices in a HMM, it is possible to state that the  
 265 harvesting process can be characterized by the following matrices:

$$A = \begin{bmatrix} 0.9153 & 0.0847 & 0.0000 & 0.0000 \\ 0.0000 & 0.8169 & 0.1831 & 0.0000 \\ 0.0000 & 0.0000 & 0.6966 & 0.3034 \\ 0.0000 & 0.0000 & 0.0000 & 1.0000 \end{bmatrix} \quad (11)$$

$$\pi = [1 \ 0 \ 0 \ 0] \quad (12)$$

266 where  $A$  is obtained by computing the expected residence time on each state in the training data set [15].  
 267 In this case,  $\pi$  is known since the HMM is always initialized in state *S1* ("Picking"). The characterization  
 268 of the entire process using a HMM allows to use the Viterbi algorithm for state transition time detection  
 269 purposes.

### 270 3.5. Proposed Methodology for Fruit Damage Indicator

271 A natural byproduct associated with the implementation of the Viterbi algorithm for estimation of the  
 272 most likely state path is that it is also possible to detect start and end times for each of the different stages  
 273 of the berry harvesting process. These start and ending times become critical information to characterize  
 274 the potential damage accumulated during "picking", "waiting", and "transport" stages since during that  
 275 lapse the fruit in the bin is exposed to higher level of vibrations and elevated temperatures. Inspired on  
 276 this fact, this research effort has proposed the following damage indicator to assess the potential damage  
 277 incurred by the fruit during the harvesting process:

$$DamageIndicator = \frac{1}{10^5} \cdot \left( \sum_{i=0}^{T_{S4}} Temp\_2_i + \sum_{i=0}^{T_{S4}} IMU\_Energy_i \right) \quad (13)$$

278 where *IMU\_Energy* is a variable that indicates the energy associated with the vibration signal recorded  
 279 by sensors in the bin during a 15[s] sliding window.  $T_{S4}$  corresponds to the moment in which the Viterbi  
 280 algorithm detects a transition from states  $S3$  to  $S4$ , measured in seconds. The temporal reference  $t = 0$  is  
 281 established to be synchronized with the start of the "picking" stage.

282 The proposed indicator for potential fruit damage offers robustness against disturbances in estimates  
 283 of transition times, since it solely depends on  $T_{S4}$  for all practical purposes. Indeed,  $T_{S4}$  determines the  
 284 start of the "cooling" stage and thus, it is expected to observe at that time simultaneous (and sudden)  
 285 drops in readings of sensors *Temp\_1* and *Temp\_2*, while the energy in the vibration signal should be small  
 286 compared to "picking" and "transport" stages. This evidence anticipates that errors in the estimate of  $T_{S4}$   
 287 should be negligible in comparison to the total time allotted for the harvesting cycle, and therefore the  
 288 value of the proposed damage indicator, which depends on the overall accumulation of stress on the fruit,  
 289 should not exhibit significant changes on its value.

#### 290 4. Obtained Results in Experimental Campaign

291 Table 1 and Figures 6-15 show the results obtained when applying the proposed scheme for harvest  
 292 stage recognition and potential fruit damage assessment on actual field data from an experimental  
 293 campaign. Each figure consists of three graphs that help to understand the manner in which the proposed  
 294 algorithm interprets the acquired data. The first graph shows the performance exhibited by the Viterbi  
 295 algorithm in the detection of transitions between each one of the first 4 stages of the harvesting process:  
 296 "picking", "wait", "transport", and "cooling". The second graph shows the energy of the IMU signal  
 297 (averaged over a 15[s] sliding window), and finally the third graph on each figure show the temperature  
 298 registered on the second temperature sensor inside the bin. Figures 6-15 are sorted in terms of the one that  
 299 represents the most potential fruit damage to the one that is more innocuous. Given the structure of the  
 300 proposed damage indicator, both the time of exposure of the fruit at ambient temperature (principally at  
 301 states  $S1$ - $S3$ ) and cumulative energy of vibration signals (principally at state  $S1$ ) have critical influence on  
 302 the assessment of potential damage.

Table 1. Experimental campaign: Harvesting cycles ordered in terms of potential fruit damage.

Harvesting cycle ( $N_i c_j$ : $bin_i$ , $cycle_j$ )	Damage Index
$N_5 c_1$	1.4762
$N_2 c_1$	1.3710
$N_1 c_1$	1.3386
$N_4 c_2$	1.3017
$N_3 c_2$	1.2905
$N_2 c_2$	1.1239
$N_1 c_2$	1.1119
$N_5 c_2$	1.0218
$N_4 c_1$	0.8002
$N_3 c_1$	0.7484

303 Figure 6 illustrates a case where the potential fruit damage is the greatest. One of the reasons  
 304 that explain this statement is the fact that in this cycle the fruit was exposed to relatively high ambient  
 305 temperature for a lengthy lapse of time. Moreover, both during the "picking" and "transport" stages, the  
 306 energy of the IMU accelerometer signal is significant, indicating that the fruit in the bin could have been

307 shaken excessively. It is important to note that the Viterbi algorithm in this case fails to detect the transition  
 308 between states  $S_1$  and  $S_2$  (overall efficacy in detection in this data set is 89.918%). Although this issue  
 309 affects the tractability of the bin in the system, it does not have an impact of the assessment of the potential  
 310 fruit damage since the transitions to  $S_4$  ("cooling stage") is perfectly detected.

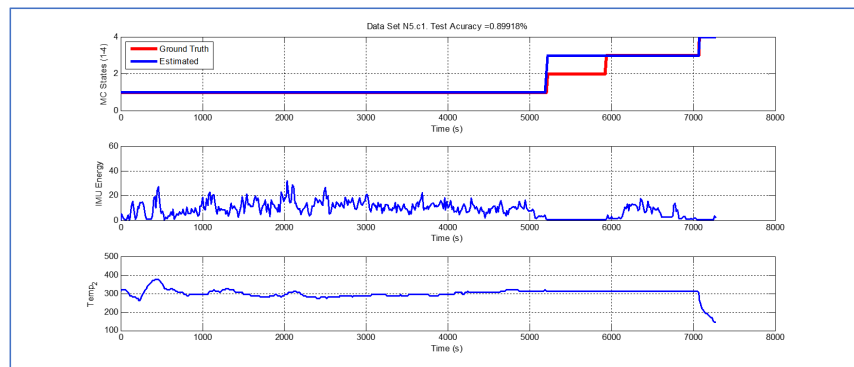


Figure 6. Detection of berry harvesting stages. Data set  $N_5c_1$

311 Figures 7-8 illustrate a case where the potential fruit damage is significantly high. Although the same  
 312 concepts explained in the previous case also apply here, it is important to note that the energy associated  
 313 to the vibration signal is lower than in the case of Figure 6. Also, please note that the performance of the  
 314 Viterbi algorithm is high (overall efficacy in detection in these data sets is 99.396%), exhibiting a negligible  
 315 delay in the detection of the transition between  $S_1$  and  $S_2$  in data set  $N_1c_1$ , being the latter used for  
 316 validation purposes of the proposed approach.

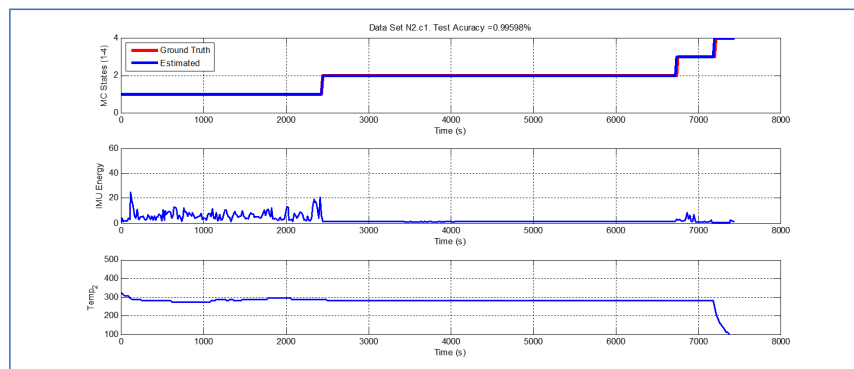
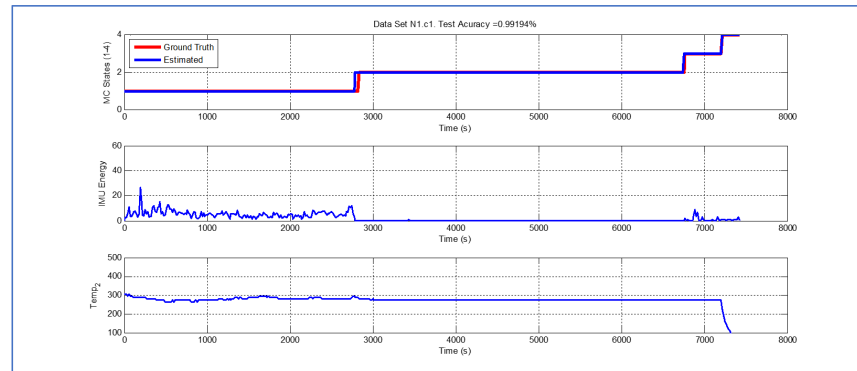
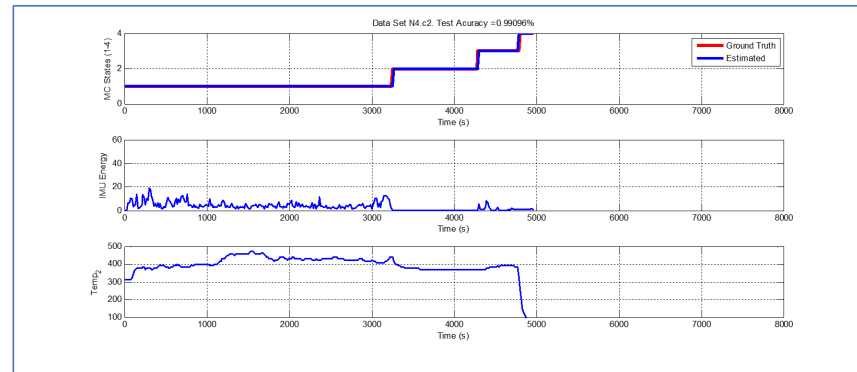


Figure 7. Detection of berry harvesting stages. Data set  $N_2c_1$



**Figure 8.** Detection of berry harvesting stages. Data set  $N_{1c1}$

317 Although temperature associated with the data shown in Figures 9 - 11 is higher than their  
 318 predecessors, the lapse of time where the fruit was exposed to ambient temperature is considerably  
 319 smaller. In both cases, there is a small delay in the estimate of parameter  $T_{S4}$ , but the performance of the  
 320 Viterbi algorithm is still beyond 98.95%.



**Figure 9.** Detection of berry harvesting stages. Data set  $N_{4c2}$

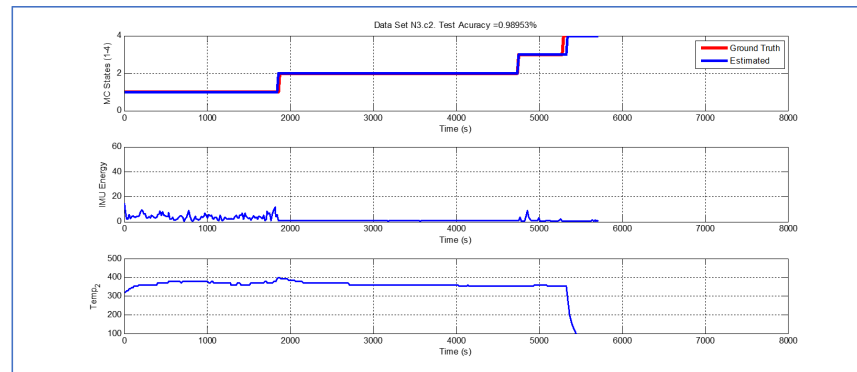


**Figure 10.** Detection of berry harvesting stages. Data set  $N_{3c2}$

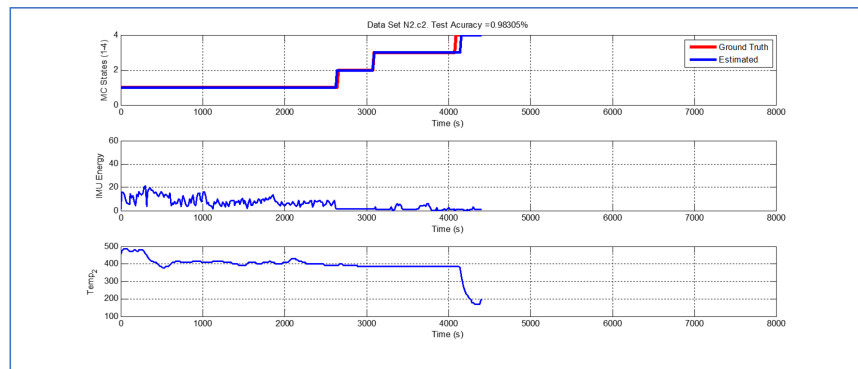


**Figure 11.** Detection of berry harvesting stages. Data set  $N_{2c2}$

321 Validation data set  $N_{1c2}$  (Figure 12) is the one where the Viterbi algorithm exhibits the lowest  
 322 performance (overall efficacy in detection in these data sets is 84.667%). Nevertheless, even in this case, the  
 323 error associated with the estimate of parameter  $T_{S4}$  is 90[s], which represents 2% in a data set that records  
 324 4485[s] of operation.

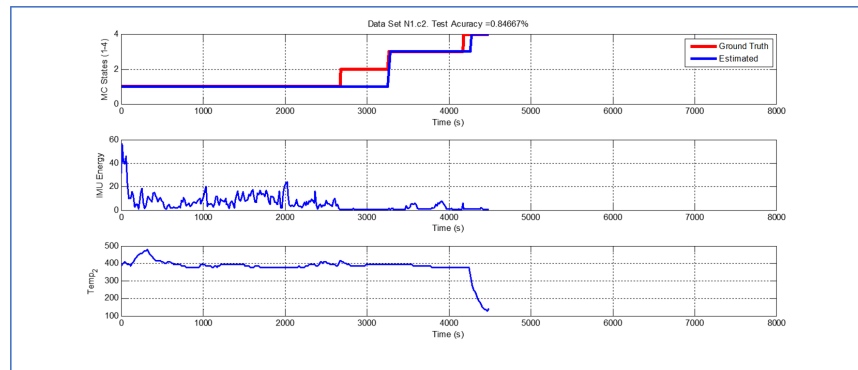


**Figure 12.** Detection of berry harvesting stages. Data set  $N_{1c2}$

325 Last but not least, Figures 13 - 15 exhibit analogous performance in terms of the accuracy of the Viterbi  
 326 algorithm. Interestingly, in terms of potential fruit damage, the most innocuous data set corresponds to  
 327 one where the ambient temperature was low, and where the harvesting cycle lasted less than 4425[s].

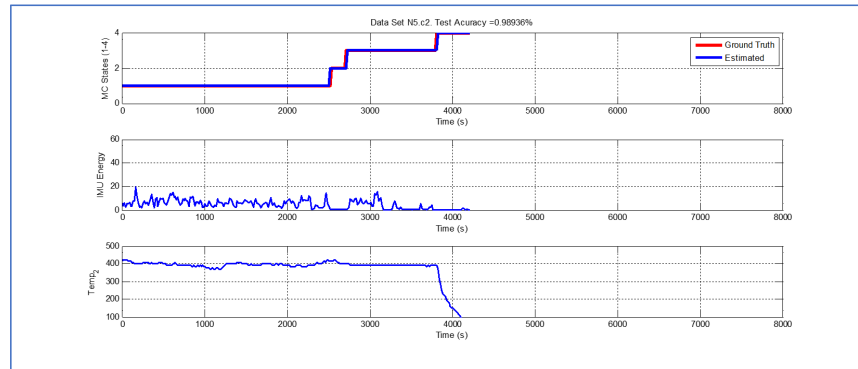


**Figure 13.** Detection of berry harvesting stages. Data set  $N_{5c2}$

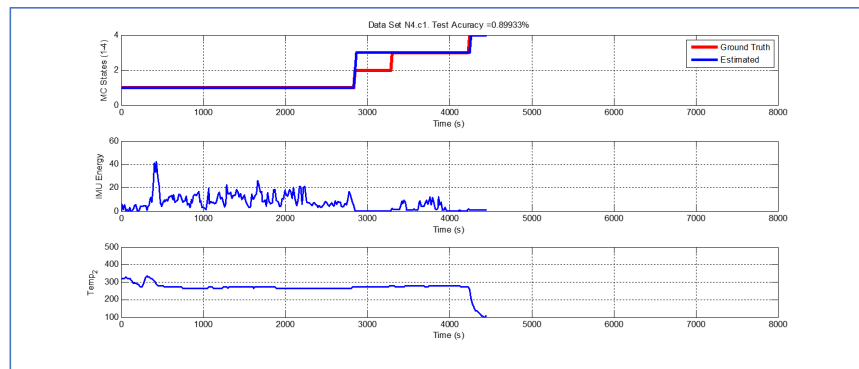


**Figure 14.** Detection of berry harvesting stages. Data set  $N_{4c1}$

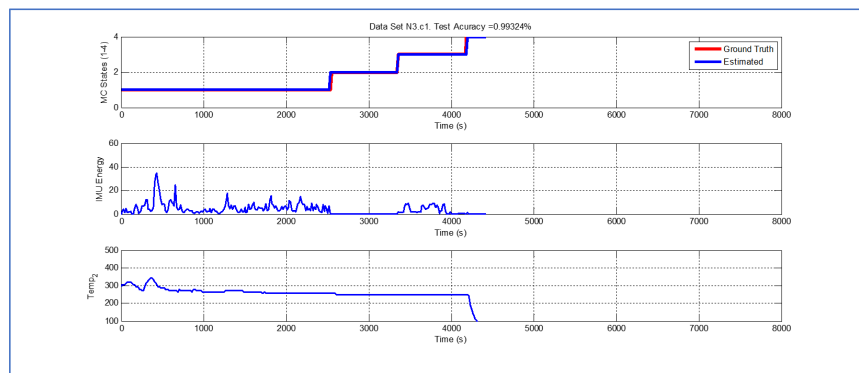


**Figure 15.** Detection of berry harvesting stages. Data set  $N_{3c1}$

## 328 5. Conclusions

329 This article proposes a monitoring system and a for berry harvesting solely based on the use of  
 330 temperature and vibration sensors. The monitoring system assumes a characterization of the process in  
 331 terms of a Hidden Markov Model and uses the Viterbi algorithm to perform inference and estimate the  
 332 most likely state trajectory.

333 The obtained state trajectory estimate is then used to compute a potential damage indicator for the  
 334 fruit in terms both of the registered temperature and vibration energy, with overall average efficacy in  
 335 detection for validation data sets of 91.937%, while errors in the estimates of the moment at which the bin  
 336 reaches the cooling stage were not larger than 2%, a fact that validates the proposed damage indicator as a  
 337 robust feature for characterization of the potential degradation in the quality of the fruit when used in  
 338 conjunction with the Viterbi algorithm for purposes of estimating the value of  $T_{S4}$ .

339 More importantly, the proposed procedure proves to be equivalent in terms of the effectiveness in  
 340 the characterization of the stages of the harvesting process to other alternatives found in the literature,  
 341 but significantly more efficient since it does not require information about the weight of the bin in which  
 342 the fruit is collected to identify the different stages of the harvesting process and determine indicators  
 343 that could help to assess if this harvesting process is being performed normally. It seems that the Viterbi  
 344 algorithm is a complex solution for this problem but is inexpensive to include those procedures in the  
 345 software running on the microprocessor of the "Smartbins", avoiding the need to measure weight and  
 346 consequently disregarding the strain gauges and the mechanical parts needed to support them. The fact  
 347 that it is possible to dispense the utilization of weight sensors in the design of "Smartbins", replacing it by  
 348 more advanced signal processing tools, has a significant economic impact in terms of the penetration of

349 these monitoring devices in the agricultural market as a right solution for some of the problems that the  
350 industry has faced over these years

351 **Author Contributions:** Project administration, P.G.; Conceptualization, C.M., M.O and P.G.; Data curation, H.R.;  
352 Formal analysis, M.O.; Investigation, P.G., C.M. and M.O.; Methodology, M.O, C.M. and P.G.; Validation, J.H.;  
353 Visualization, M.O.; Writing—original draft, C.M and M.O.; Writing—review & editing, C.M and M.O.

354 **Funding:** This work has been supported by the FONDEF IDeA Project ID16I10206 and also by the Advanced Center  
355 for Electrical and Electronic Engineering, AC3E, Basal Project FB0008, CONICYT.

356 **Conflicts of Interest:** The authors declare no conflict of interest.

## 357 References

- 358 1. Muñoz, M. Boletín frutícola avance Octubre 2018. *Oficina de Estudios y Políticas Agrarias (Odepa) del Ministerio  
359 de Agricultura, Gobierno de Chile* **2018**.
- 360 2. Li, Z.; Thomas, C. Quantitative Evaluation of Mechanical Damage to Fresh Fruits. *Trends in Food Science &  
361 Technology* **1991**, *32*, 138–150. doi:10.1016/j.tifs.2013.12.001.
- 362 3. Aliasgarian, S.; Ghassemzadeh, H.; Moghaddam, M.; Ghaffari, H. Mechanical Damage of Strawberry  
363 during Harvest and Postharvest Operations. *World Applied Sciences Journal* **2013**, *22*, 969–974.  
364 doi:10.5829/idosi.wasj.2013.22.07.798.
- 365 4. Vergano, P.; Testin, R.; Newall, C. Distinguishing among Bruises in Peaches Caused by Impact, Vibration, and  
366 Compression. *Journal of Food Quality* **1991**, *14*, 285–298. doi:10.1111/j.1745-4557.1991.tb00069.x.
- 367 5. Lin, X.; Brusewitz, G. Peach Bruise Thresholds Using the Instrumented Sphere. *Applied Engineering in  
368 Agriculture* **1994**, *10*, 509–513. doi:10.13031/2013.25880.
- 369 6. Sanford, K.; Lidster, P.; McRae, K.; Jackson, E.; Lawrence, R.; Stark, R.; Prange, R. Lowbush Blueberry Quality  
370 Changes in Response to Mechanical Damage and Storage Temperature. *Journal of the American Society for  
371 Horticultural Science* **1991**, *116*, 47–51. doi:10.21273/JASHS.116.1.47.
- 372 7. Martínez-Romero, D.; Serrano, M.; Carbonell, A.; Castillo, S.; Riquelme, F.; Valero, D. *Production Practices and  
373 Quality Assessment of Food Crops*; Kluwer Academic Publishers, 2004; chapter Mechanical Damage During Fruit  
374 Post-harvest Handling: Technical and Physiological Implications, pp. 233–252.
- 375 8. Gallardo, R.K.; Stafne, E.T.; DeVetter, L.W.; Q. Zhang, C.L.; Takeda, F.; Williamson, J.; Yang, W.Q.; Cline,  
376 W.O.; Beaudry, R.; Allen, R. Blueberry Producers' Attitudes toward Harvest Mechanization for Fresh Market.  
377 *HortTechnology* **2018**, *28*, 10–16. doi:10.21273/HORTTECH03872-17.
- 378 9. Moggia, C.; Graell, J.; Lara, I.; González, G.; Lobos, G.A. Firmness at Harvest Impacts Postharvest Fruit  
379 Softening and Internal Browning Development in Mechanically Damaged and Non-damaged Highbush  
380 Blueberries (*Vaccinium corymbosum* L.). *Front. Plant Sci* **2017**, *8*, 1–11. doi:10.3389/fpls.2017.00535.
- 381 10. Timm, J.; Bollen, A.; Rue, B.D.; Woodhead, I. Apple Damage and Compressive Forces in Bulk Bins During  
382 Orchard Transport. *Applied Engineering in Agriculture* **1998**, *14*, 165–172. doi:10.13031/2013.19366.
- 383 11. Swedberg, C. Driscoll's Monitors Its Berry Shipments in Real Time. *RFID J.* **2010**, p. 1–2.
- 384 12. Ampatzidis, Y.G.; Vougioukas, S.G.; Whiting, M.D. A wearable module for recording worker position in  
385 orchards. *Comput. Electron. Agric.* **2011**, *78*, 222–230. doi:10.1016/j.compag.2011.07.011.
- 386 13. Ampatzidis, Y.; Whiting, M.; Scharf, P.; Zhang, Q. Development and evaluation of a novel system for monitoring  
387 harvest labor efficiency. *Comput. Electron. Agric.* **2012**, *88*, 85–94. doi:10.1016/j.compag.2012.06.009Get.
- 388 14. Galeas, P.; Muñoz, C.; Huircan, J.; Fernandez, M.; Segura-Ponce, L.A.; Duran-Faundez, C. Smartbins:  
389 Using Intelligent Harvest Baskets to Estimate the Stages of Berry Harvesting. *Sensors* **2019**, *19*, 1361.  
390 doi:10.3390/s19061361.
- 391 15. Rabiner, L.R. A tutorial on hidden Markov models and selected applications in speech recognition. *Proceedings  
392 of the IEEE* **1989**, *77*, 257–286. doi:10.1109/5.18626.
- 393 16. Viterbi, A. Error bounds for convolutional codes and an asymptotically optimum decoding algorithm. *IEEE  
394 transactions on Information Theory* **1967**, *13*, 260–269. doi:10.1109/TIT.1967.1054010.
- 395 17. Forney, G.D. The viterbi algorithm. *Proceedings of the IEEE* **1973**, *61*, 268–278.

<sup>396</sup> 18. *The Viterbi Algorithm*, 2009. doi:10.1007/978-0-387-73003-5\_592.

<sup>397</sup> **Sample Availability:** Samples of the compounds ..... are available from the authors.